Continued Analysis of *EUVE* and Optical Observations of a Flare on AD Leonis

S. L. CULLY[1,2] G. H. FISHER,[1] S. L. HAWLEY,[3] AND T. SIMON[4]

[1] Experimental Astrophysics Group, Space Sciences Laboratory, University of California, Berkeley CA 94720 USA

[2] Center for Extreme Ultraviolet Astrophysics, 2150 Kittredge Street, University of California, Berkeley, CA 94720-5030, USA

[3] Department of Physics and Astronomy, Michigan State University, East Lansing, MI 48824, USA

[4] Institute for Astronomy, University of Hawaii, 2680 Woodlawn Dr., Honolulu, HI 96822, USA

The flare star AD Leo (dM3.5e, 4.9 pc) was observed by *EUVE* from 1993 March 1–March 3 UT. A flare was detected by the *EUVE* DS/S and seen in optical photometry on 1993 March 2 UT. We summarize an analysis of the flare's physical parameters, and present differential emission measure (DEM) curves calculated for the quiescent, flare peak and flare decay phases of the observation.

The flare star AD Leo (dM3.5e, 4.9 pc) was observed by the *EUVE* DS/S from 1993 March 1–March 3 UT. Two flares were clearly visible in the lightcurve of the Lexan/boron (40–190 Å) band of the Deep Survey Instrument (Fig. 1) occurring March 2 and 3 UT. The impulsive phase at the beginning of the larger flare (Flare 1 in Fig. 1) was also observed with optical photometry at Lick Observatory (Fig. 2). The 0.6 magnitude optical U band (3000–4300 Å) flare had a peak DS Lex/B count rate of 1.0 cps and was visible for 7 hours. Hawley et al. (1995) estimated the total EUV energy released during the 7 hour peak of the larger flare to be $\sim 2 \times 10^{33}$ ergs. Using the stellar flare loop model developed by Fisher & Hawley (1990), Hawley et al. (1995) found that the flare could be modeled as a constant area loop with a half length of 4×10^{10} cm ($\sim R_*$), a coronal cross sectional area of 9×10^{19} cm^2 and an average electron density of 3×10^{10} cm^{-3}. They also used the contemporaneous optical data taken in the Johnson U, B and V bands during the flare to compute a photospheric fractional stellar area coverage of 0.01% (1×10^{18} cm^2) and a blackbody temperature of 9000 K. ($T_{\rm eff} \sim 3000$ K during quiescence).

In Fig. 3, we show that the *EUVE* DS Lex/B and optical U Band (3000–4300 Å) luminousities roughly follow the relation, $L_{\rm EUV} \propto \int_0^t L_{\rm U}\, dt'$ during the impulsive phase of the EUV flare Hawley et al. (1995). This is reminiscent of the Solar "Neupert" effect where the EUV and Soft X Ray emission from hot, evaporated, chromospheric material in the flare loop(s) is seen to be proportional to the time integral of the Hard X-ray and white light emission (Neupert (1968), Dennis & Zarro (1993)).

Figure 4 shows the optimally extracted, fluxed *EUVE* (60–600 Å) spectra taken during quiescence, the peak of the large flare and the "tail" between the two flares (see Fig. 1). Figure 5 and Table 1 show the results of two different methods of estimating the volume differential emission measure (DEM) ($n_e{}^2$dV/dln(T)) of the emitting plasma during each of the time periods mentioned above. Both methods assumed a column density of 2×10^{18} cm^{-2} and used the updated Landini and Mosignori-Fossi plasma line list (Monsignori Fossi & Landini (1994)) in the low density limit. Abundances 0.4 dex lower than Solar coronal abundances (Naftilan, Sandmann & Pettersen (1992)) were also assumed.

S. Bowyer and R. F. Malina (eds.), Astrophysics in the Extreme Ultraviolet, 153–158.

https://doi.org/10.1017/S0252921100035892 Published online by Cambridge University Press

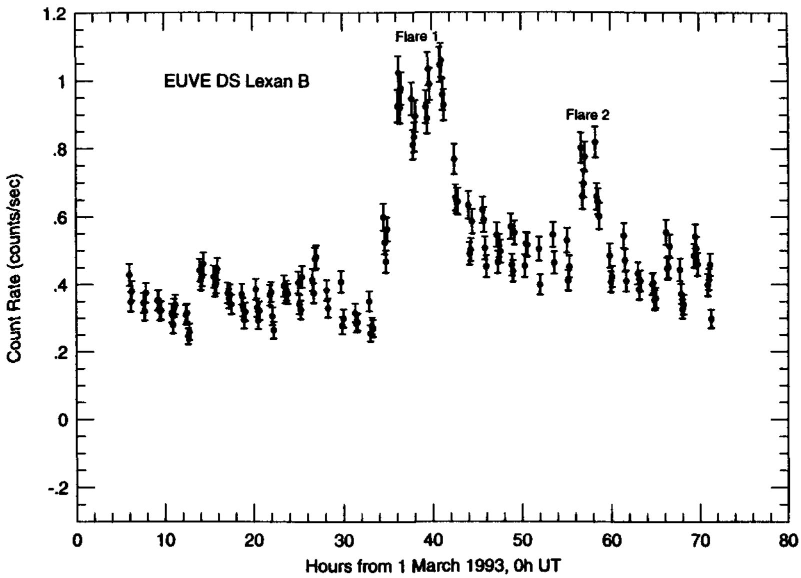

FIGURE 1. EUVE DS Lex/B Lightcurve

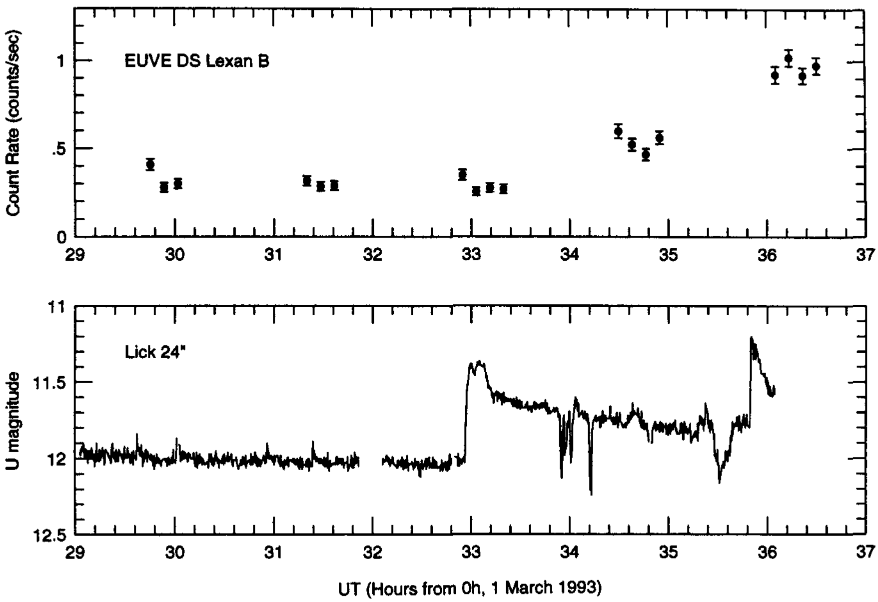

FIGURE 2. EUVE DS Lex/B and optical U band lightcurves at the onset of the large flare shown in Fig. 1.

https://doi.org/10.1017/S0252921100035892 Published online by Cambridge University Press

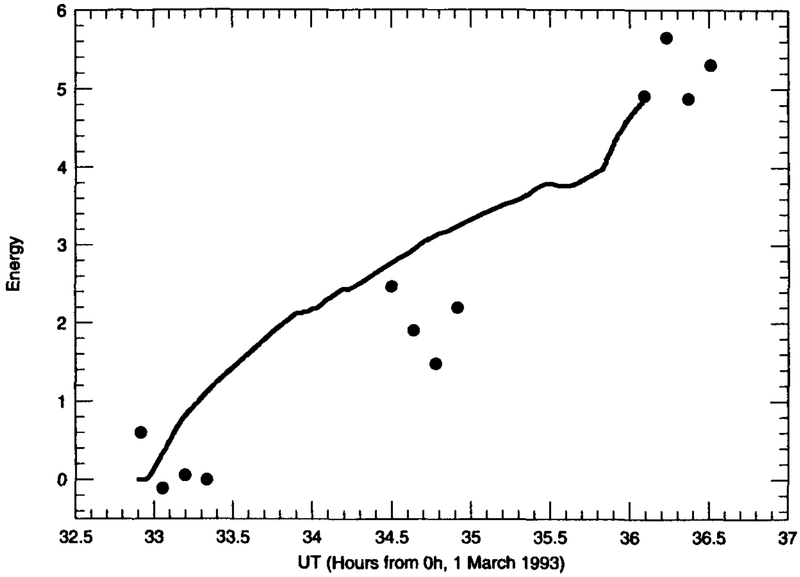

FIGURE 3. Illustration of the Neupert effect calculated from the data shown in Fig. 2; — U-band ergs, * 10^{-32}, • *EUVE* DS, - ergs–s^{-1}, * (3×10^{-27})

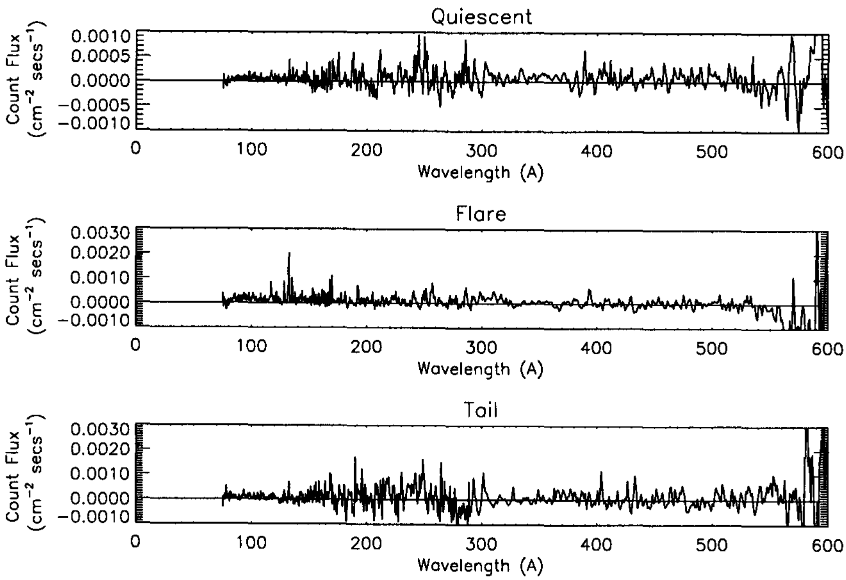

FIGURE 4. Fluxed Spectra taken during the peak of the large flare, the "tail" between the two flares and Quiescence

https://doi.org/10.1017/S0252921100035892 Published online by Cambridge University Press

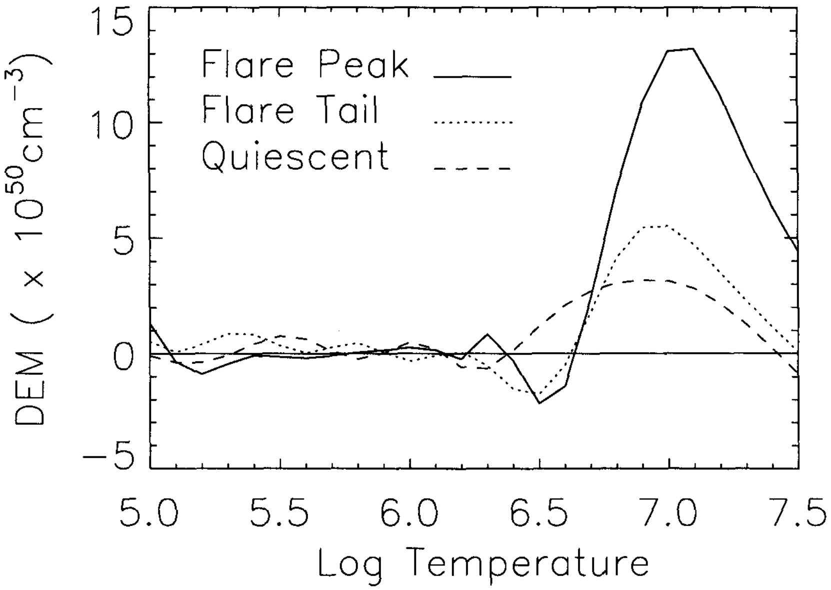

FIGURE 5. DEM analysis for the spectra shown in Fig. 4

Table 1 shows the results of a differential emission measure (DEM) analysis using unblended single lines. In the cases, where a positive detection is shown the line was detected with a certainty of at least 2 σ. Each DEM value was calculated by using the formula

$$DEM(T_{\rm Max}) = \frac{4\pi d^2 f_{\rm obs}}{\int \epsilon(T')\, dT'}$$

where $\epsilon(T)$ is the line power output as a function of temperature at our assumed elemental abundance, d is the distance to the source, $f_{\rm obs}$ is the observed line flux and $T_{\rm Max}$ is the peak line power temperature.

Figure 5 shows the continuous DEMs found using an inversion procedure similar to that described in Craig & Brown (1986) and Mewe et al. (1995). In this method, the entire spectrum is used, as opposed to just a few lines. This increases the S/N and allows analysis of heavily blended spectra where there are no obvious single unblended lines available for separate analysis. It also finds a shape for the DEM consistent with each of the single line points when the lines are strong (e.g. around Log $T \sim 7.0$ in Table 1). However, when a spectrum is dominated by noise a single strong line can give an improved upper limit (e.g. Fe IX/O V 171.1 Å, Log $T \sim 5.8$). The inversion method can also oscillate or produce spurious high temperature tails when there is insufficient data to constrain the solution. Therefore it is desirable to use both methods to gain a more accurate picture.

Figure 5 and Table 1 show that the spectra in all three cases are dominated by the high temperature ($\sim 10^7$ K) Fe lines. The curves show progressively cooler peak temperatures

https://doi.org/10.1017/S0252921100035892 Published online by Cambridge University Press

TABLE 1. Summary of Differential Emission Measures Calculated from Individual Spectral Lines

Lambda (Å)	Ion	Log T (K)	Log Quiescent DEM (cm^{-3})	Log Flare Peak DEM (cm^{-3})	Log Flare Tail DEM (cm^{-3})
192.0	Fe XXIV	7.2	< 50.9	< 51.1	—
255.1	Fe XXIV	7.2	< 51.3	< 51.6	< 51.8
132.9	Fe XXIII/XX	7.2	50.6	51.4	50.8
135.8	Fe XXII	7.1	51.0	51.5	< 51.2
116.3	Fe XXII	7.1	< 51.1	< 51.5	< 51.4
117.2	Fe XXII	7.1	51.0	51.6	< 51.2
118.2	Fe XX/XXI	7.0	< 51.1	51.4	< 51.4
121.6	Fe XX	7.0	< 50.8	51.3	< 51.1
128.7	Fe XXI	7.0	50.6	51.4	50.9
108.4	Fe XIX	6.9	50.9	51.3	51.0
93.7	Fe XVIII	6.8	50.7	51.2	51.2
334.2	Fe XVI	6.4	50.4	< 50.4	< 50.5
284.1	Fe XV	6.3	50.1	< 50.1	< 50.4
202.0	Fe XIII	6.2	< 49.7	< 49.9	< 50.2
181.2	Fe XI	6.1	< 49.8	< 50.6	< 50.6
196.6	Fe XII	6.1	< 49.9	< 50.0	< 50.5
174.5	Fe X	6.0	< 50.0	< 49.8	< 50.0
177.2	Fe X	6.0	< 49.9	< 50.7	< 50.6
171.1	Fe IX/O V	5.9	49.2	< 49.1	< 49.5
401.7	Ne VI	5.7	< 50.3	< 50.4	< 50.6
358.9	Ne V	5.5	< 50.4	< 50.5	< 50.6
238.5	O IV	5.3	< 49.9	< 50.0	< 50.4
554.4	O IV	5.3	< 49.5	< 49.7	< 49.9
303.7	He II	4.9	< 49.7	< 50.0	< 50.0

and smaller emission measures as the flare evolves from its peak, through the decay tail and back to quiescence. This behavior is suggestive of a general cooling of the flare loops but may also be due to the superposition of progressively cooler flaring events.

REFERENCES

CRAIG, I. J. D. & BROWN, J. C., EDS. 1986, Inverse problems in astronomy: A guide to inversion strategies for remotely sensed data, Bristol: Adam Hilger Ltd.

CULLY, S. L. ET AL. 1995, EUVE spectral observations of a flare on AD Leonis, in preparation

DENNIS, B. R. & ZARRO, D. M. 1993, The Neupert effect—What it can tell us about the impulsive and gradual phases of solar flares, Sol. Phys., 146, 177

FISHER, G. H. & HAWLEY, S. L. 1990, An equation for the evolution of solar and stellar Flare Loops, ApJ, 357, 243

HAWLEY, S. L., ET AL. 1995, Simultaneous EUVE and optical observations of AD Leonis: Evidence for large coronal loops and the Neupert effect in stellar flares, ApJ, in press

MONSIGNORI, FOSSI, B. C. & LANDINI, M. 1994, The X-Ray–EUV Spectrum of Optically Thin Plasmas, Solar Phys., 152, 81

MEWE, R., ET AL. 1995, EUV spectroscopy of cool stars: 1. The corona of Alpha Centauri observed with EUVE, A&A, 296, 477

NEUPERT, W. M. 1968, Comparison of Solar X-ray line emission with microwave emission

during flares, ApJ, 153, L59
NAFTILAN, S. A., SANDMANN, W. S. & PETTERSEN, B. R. 1992, The spectrum of the dwarf Me flare star AD Leonis, PASP, 104, 1045

https://doi.org/10.1017/S0252921100035892 Published online by Cambridge University Press